Supplementary Materials

S1. Human climate exposure indices (Thom 1959, Sohar et al. 1963, Epstein et al. 2006, Buzan et al. 2014, Maia-Silva et al. 2020)

- Dew point temperature: $T_d = T - (\frac{100 - RH}{5})$, where T is the ambient air temperature and RH the relative humidity
- Wet bulb temperature :
$T_w = T \times arctan(0.151977 \times (RH + 8.313659)^{1/2}) + arctan(T + RH)$
$-arctan(RH - 1.676331) + 0.00391838 \times j^{3/2} \times arctan(0.023101 \times j) - 4.686035$
- Discomfort Index with T in degrees Celsius: $DI = 0.5T_w + 0.5T$
- Humidex : $Hx = T + \frac{5}{9}(\frac{e_{RH}}{100} - 10)$
- Heat Index :
$-42.379 + 2.04901523 \times T_f + 10.14333127 \times RH - 0.22475541 \times T_f \times RH$
$-6.83783 \times 10^{-3} \times T_f^2 - 5.481717 \times 10^{-2} \times RH^2 + 1.22874 \times 10^{-3} \times T_f^2 \times RH$
$+8.5282 \times 10^{-4} \times T_f \times RH^2 - 1.99 \times 10^{-6} \times T_f^2 \times RH^2$ Where T_f is the ambient air temperature in Fahrenheit degrees

S2. Table referencing power companies in Japan

Region	Company	Website	Type of energy supply
Hokkaido	Hokkaido Electric Power Co., Inc.	http://www.hepco.co.jp/english/	Fossil fuel, Biothermal, Photovoltaic, Wind Hydroelectricity, Geothermal, PSH
Tohoku	Tohoku Electric Power Co., Inc	https://www.tohoku-epco.co.jp/english/	Fossil fuel, Biothermal, Photovoltaic, Wind Hydroelectricity, Geothermal, PSH
Tokyo	Tokyo Electric Power Company Holdings	https://www.tepco.co.jp/en/hd/index-e.html	Fossil fuel, Biothermal, Photovoltaic, Wind Hydroelectricity, PSH
Hokuriku	Hokuriku Electric Power Company	https://www.rikuden.co.jp/english/	Fossil fuel, Biothermal, Photovoltaic, Wind Hydroelectricity, PSH
Kansai	Kansai Electric Power Co., Inc.	https://www.kepco.co.jp/english/	Fossil fuel, Photovoltaic, Wind Hydroelectricity, PSH, Nuclear

Region	Company	Website	Type of energy supply
Chubu	CHUBU Electric Power, Inc.	https://www.chuden.co.jp/english/	Fossil fuel, Photovoltaic, Wind Hydroelectricity, PSH
Shikoku	YONDEN Shikoku Electric Power CO.,Inc.	https://www.yonden.co.jp/english/index.html	Fossil fuel, Biothermal, Photovoltaic, Wind Hydroelecitricty, PSH, Nuclear
Chugoku	The Chugoku Electric Power co.,inc	https://www.energia.co.jp/e/	Fossil fuel, Biothermal, Photovoltaic, Wind Hydroelectricity, PSH
Kyushu	KYUSHU ELECTRIC POWER CO., INC.	https://www.kyuden.co.jp/english_index.html	Fossil fuel, Biothermal, Photovoltaic, Wind Hydroelectricity, Geothermal, PSH, Nuclear
Okinawa	The Okinawa Electric Power Company, Inc.	http://www.okiden.co.jp/en/	Fossil fuel, Biothermal, Photovoltaic, Wind Hydroelectricity

Table S1. List of power companies in Japan and their website. PSH = Pumped Storaged Hydroelectricity

S2. Model development and selection

	In-R2	Out-R2	In-MAPE	Out-MAPE	In-RMSE	Out-RMSE
			Power Demand (MWh)			
Random Forest	0.98	0.83	0.01	0.04	5041	13762
Gradient Boosting	0.79	0.76	0.05	0.05	15648	16773
MARS	0.97	0.84	0.01	0.04	5264	13579
			Carbon Intensity (gCO_2eq/kWh)			
Random Forest	0.91	0.32	0.03	0.07	17	45
Gradient Boosting	0.38	0.31	0.07	0.07	44	45
MARS	0.91	0.26	0.03	0.07	17	46

Table S2. Algorithm evaluation metric, average of the ten regions. “In” are for the training dataset and “Out” for the test dataset.

Note that the average daily power demand per inhabitant varies from 10 to 50 kWh across months and regions, and the carbon intensity from 400 to 700 gCO2eq/kWh.

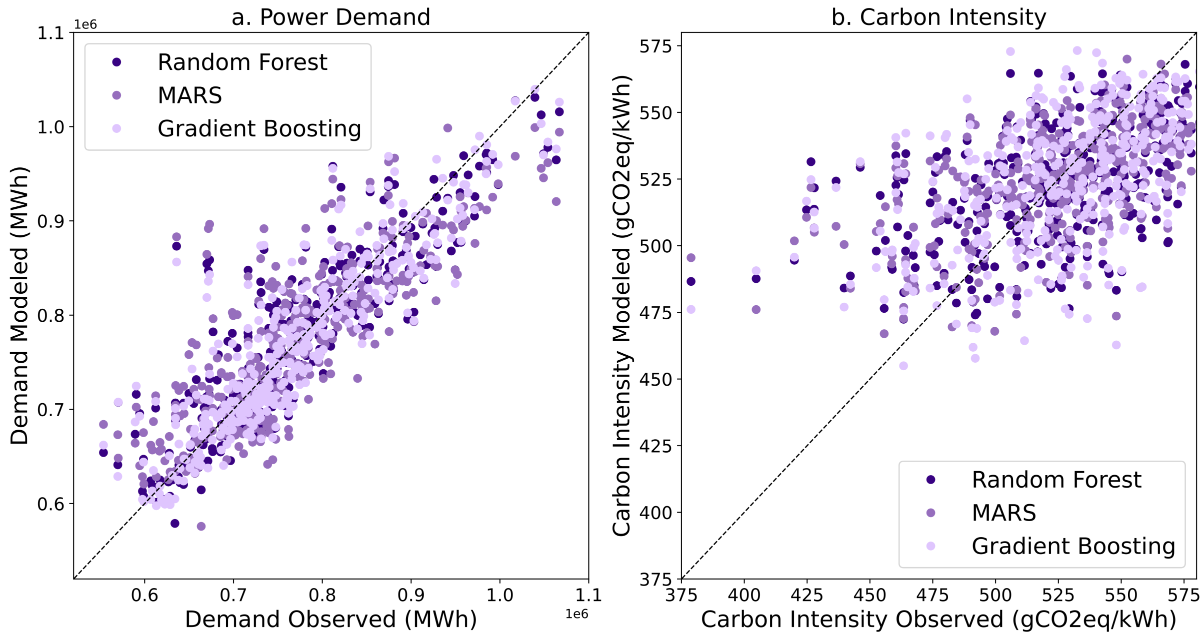

Figure S1. Scatter plots of power demand (a) and carbon intensity (b) modeled as a function of the demand observed for the test sample. Blue circles represent the results obtained with the random forest method, orange with the MARS, and green with the gradient boosting. The results shown here are for the Tokyo region.

S4. Calculation of carbon intensity projection

The carbon intensity of power generation was calculated by dividing the CO_2 emissions from power generation by the power generation from the IMAGE 3.2 model (Van Vuuren et al. 2021). The regional carbon intensity projections were also obtained, assuming the current ratios will hold over this century. For SSP370 and SSP585, we use the projections for the baseline scenarios since the forcing reaches a very high level at the end of this century. For SSP1, we use the average of four scenarios from the IMAGE 3.2 model: SSP1_SPA1_26I_D, SSP1_SPA1_26I_LI, SSP1_SPA1_26I__RE, and SSP1_SPA1_26I_LIRE. These four scenarios integrate negative emissions from carbon sequestration with BECCS (BioEnergy with Carbon Capture and Storage). As we do not assume BECCS implementation in our SSP126 scenario, we calculate the carbon intensity of power generation without considering the negative emissions. Assuming linear relationships between power demand and population and between power demand and GDP, we independently calculated the evolution of demand related to the evolution of these two factors.

S5. Partial dependence plots and Shapley Values for all regions

S2a. Hokkaido

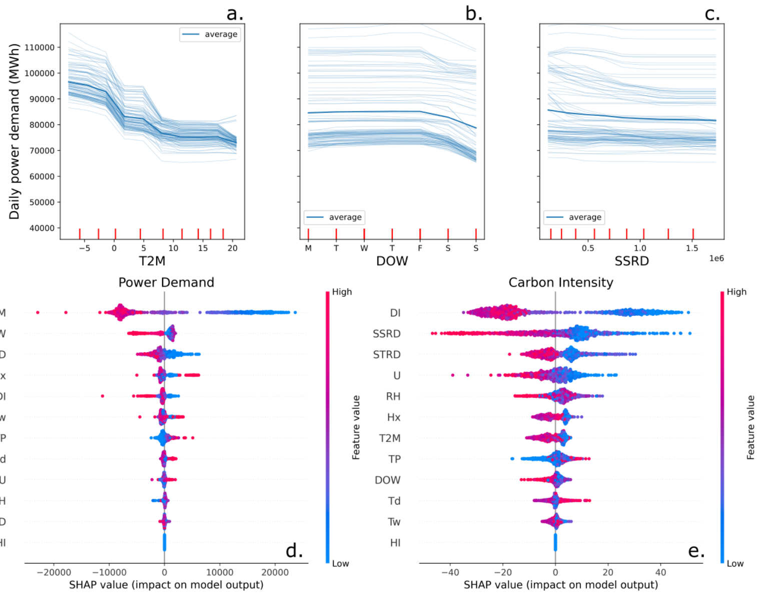

S2b. Tohoku

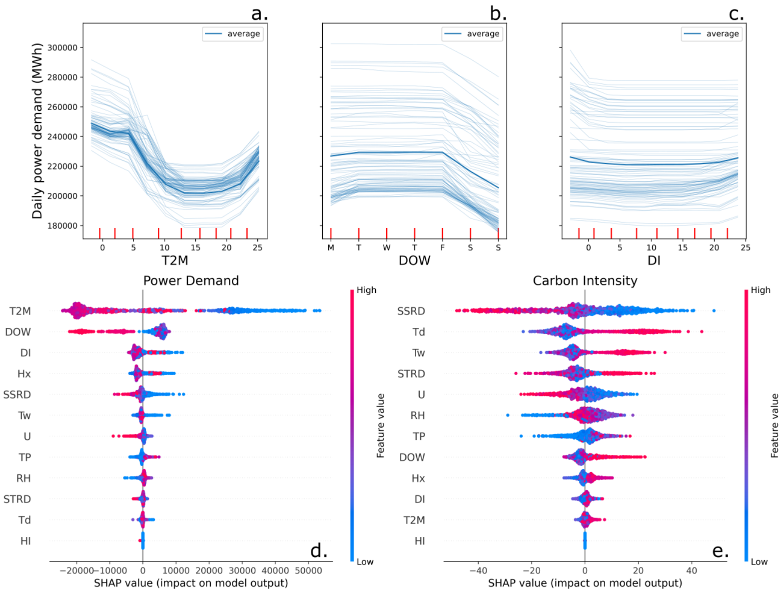

S2c. Hokuriku

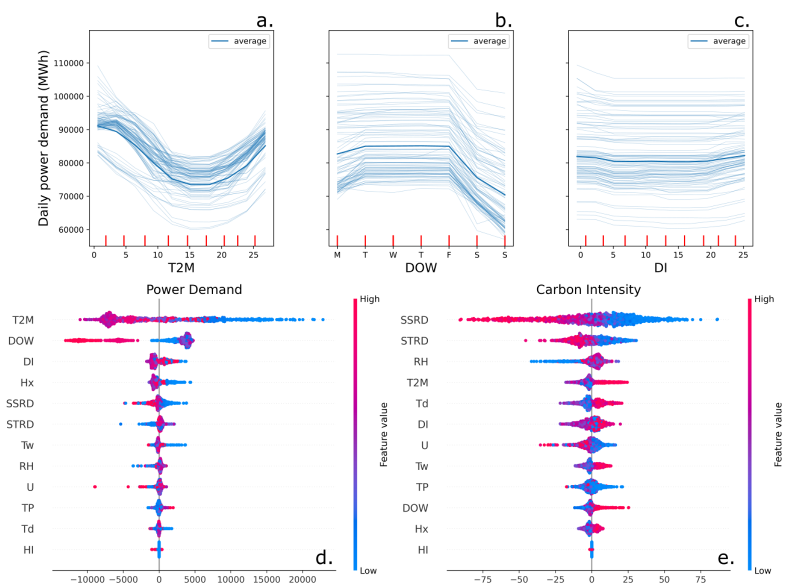

S2d. Tokyo

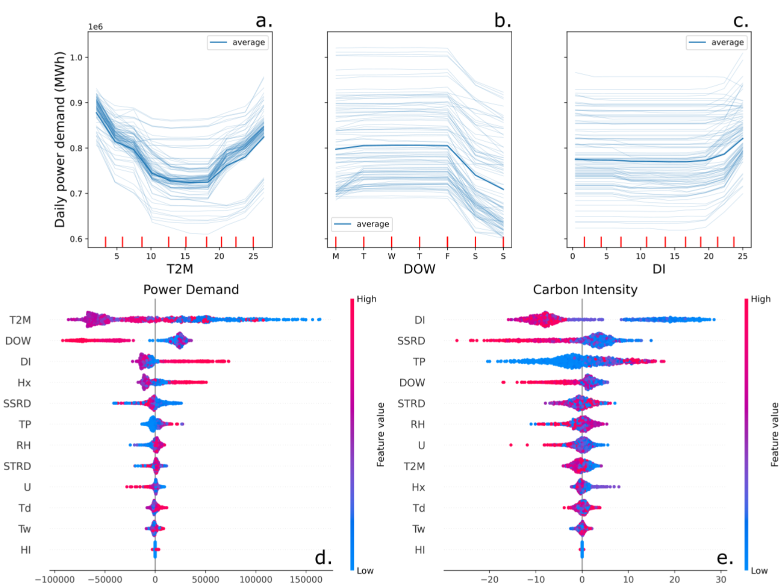

S2e. Chubu

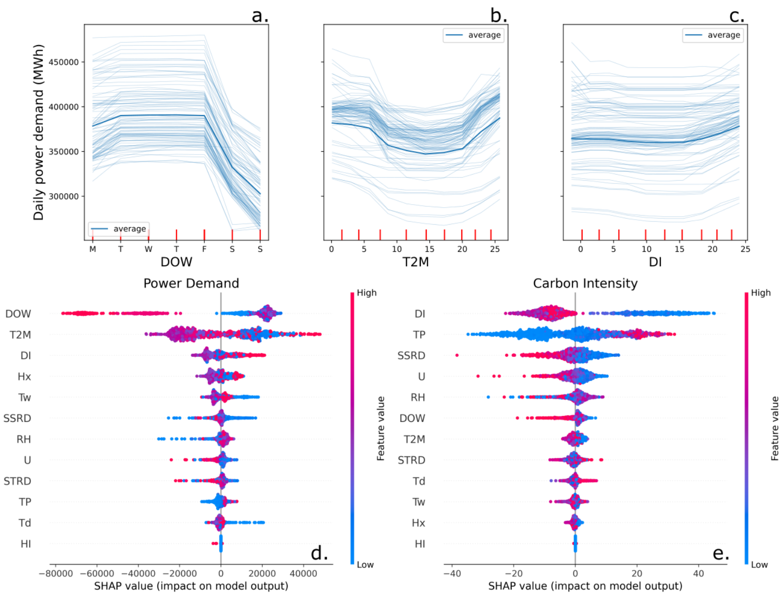

S2f. Kansai

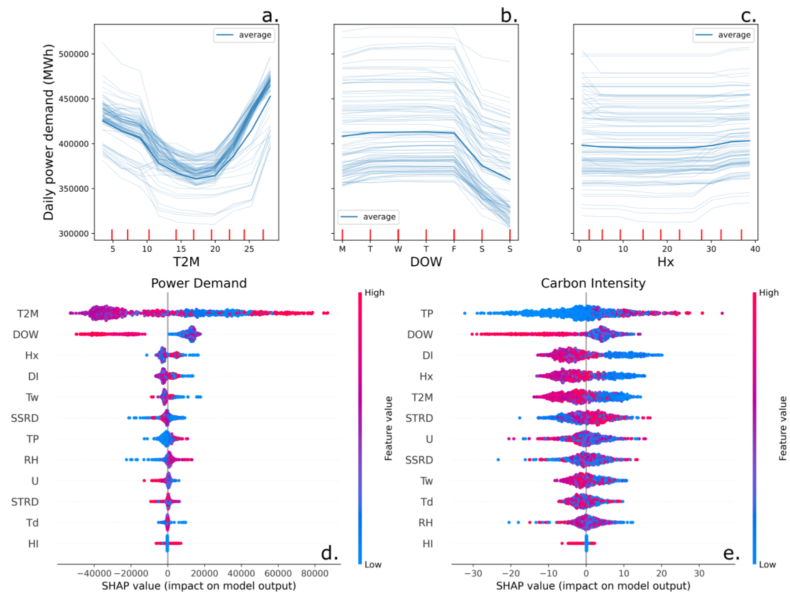

S2g. Chugoku

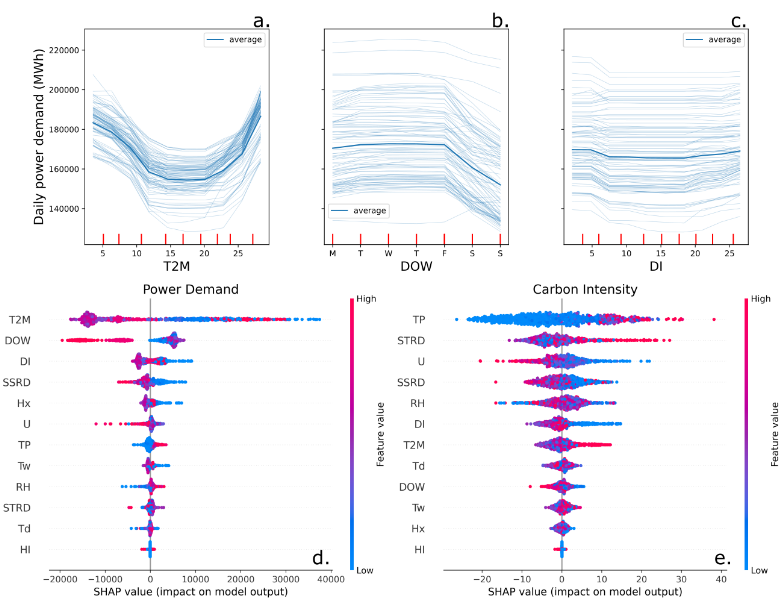

S2h. Shikoku

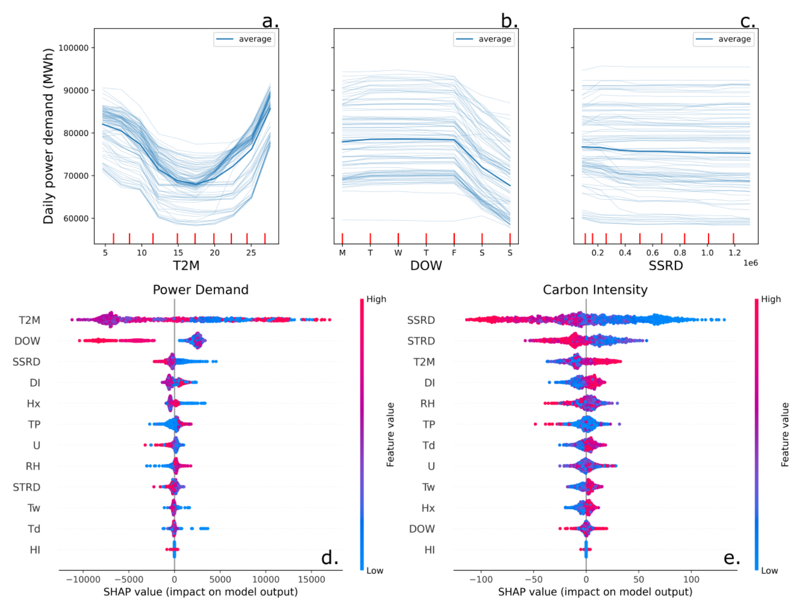

S2i. Kyushu

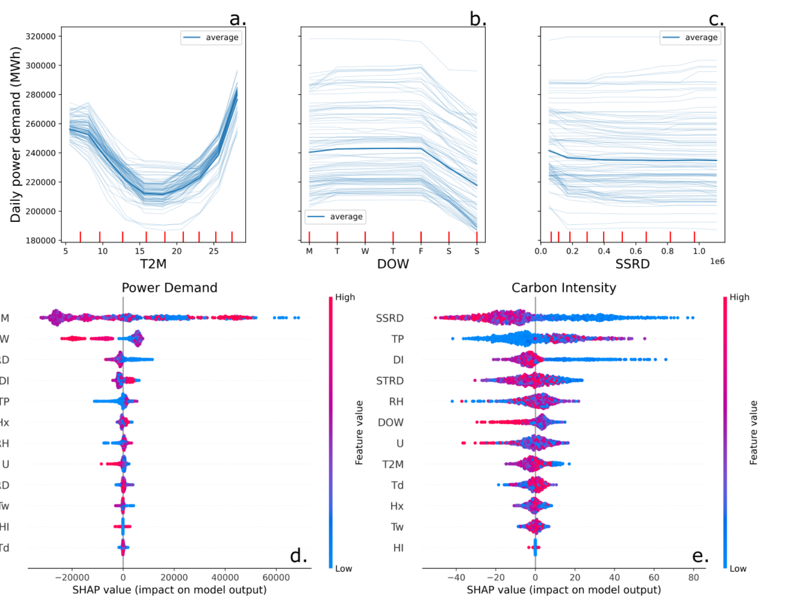

S2j. Okinawa

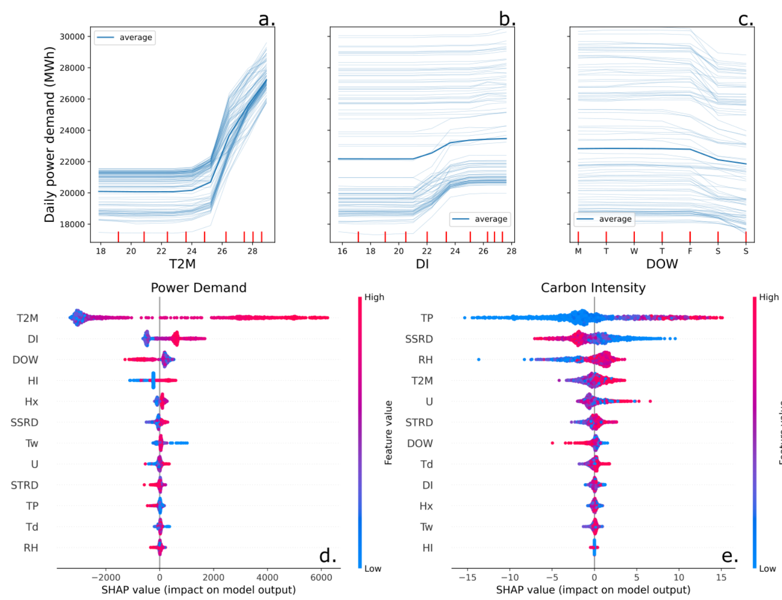

Figure S2a-j. Partial dependence plot (thick line) and Individual Conditional Expectation plots (thin lines) for 100 observations for the three main predictors explaining the power demand in the ten studied regions. For the predictor DOW, the letters indicate the days of the week. The vertical red bars show the dataset's predictor values distribution. The lower panels represent the Shapley values for each predictor and each observation for power demand (d) and carbon intensity (e) for all regions.

S6. CO_2 emissions with and without climate change effect

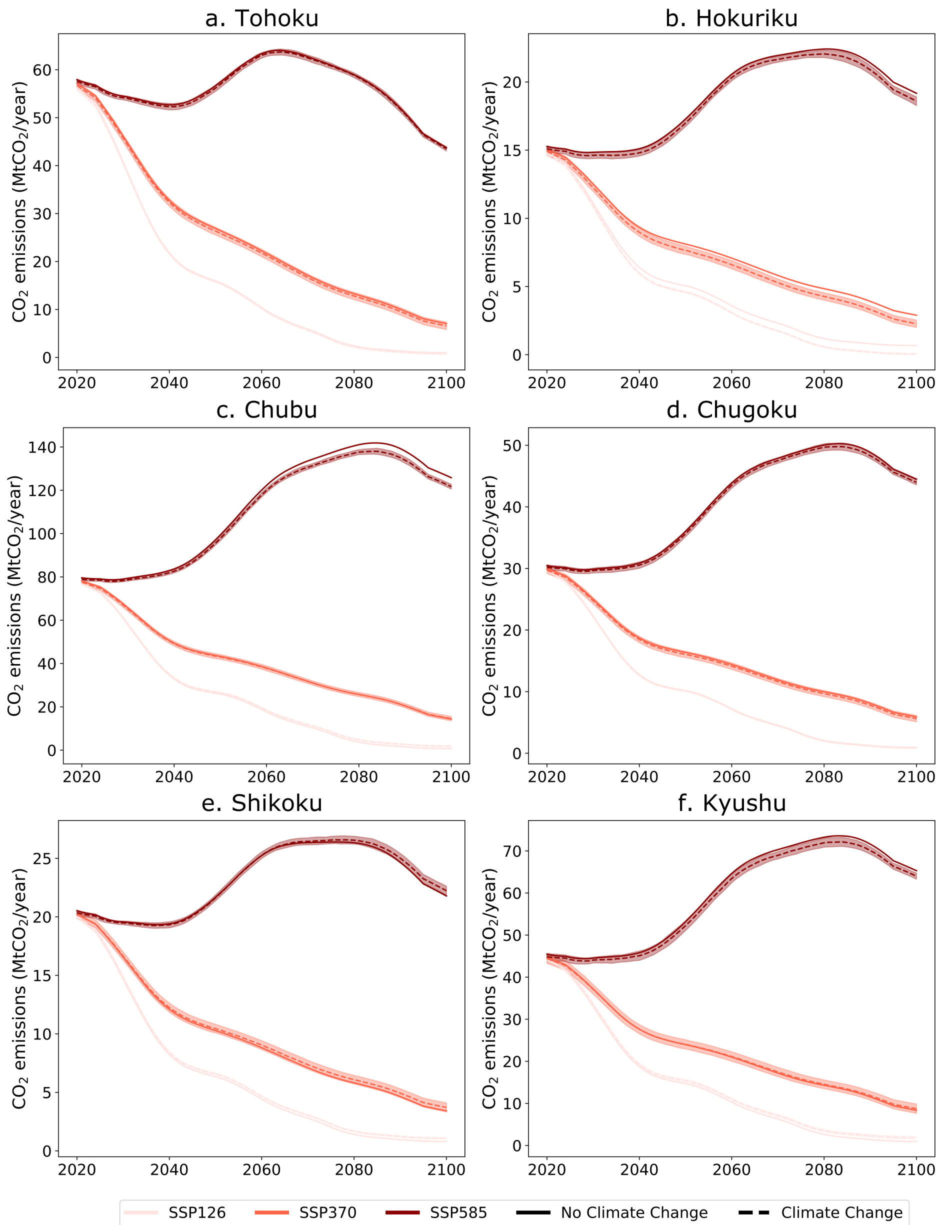

Figure S3. Annual CO_2 emissions from power production under SSP126, SSP370, and SSP585, after taking into account the effect of socio-economic factors with (dashed line) and without (direct line) the effect of climate change for six regions: Tohoku (a), Hokuriku (b), Chubu (c), Chugoku (d), Shikoku (e) and Kyushu (f). The shaded area represents the 1-sigma standard deviation from the five climate models for the climate-change effect curves.

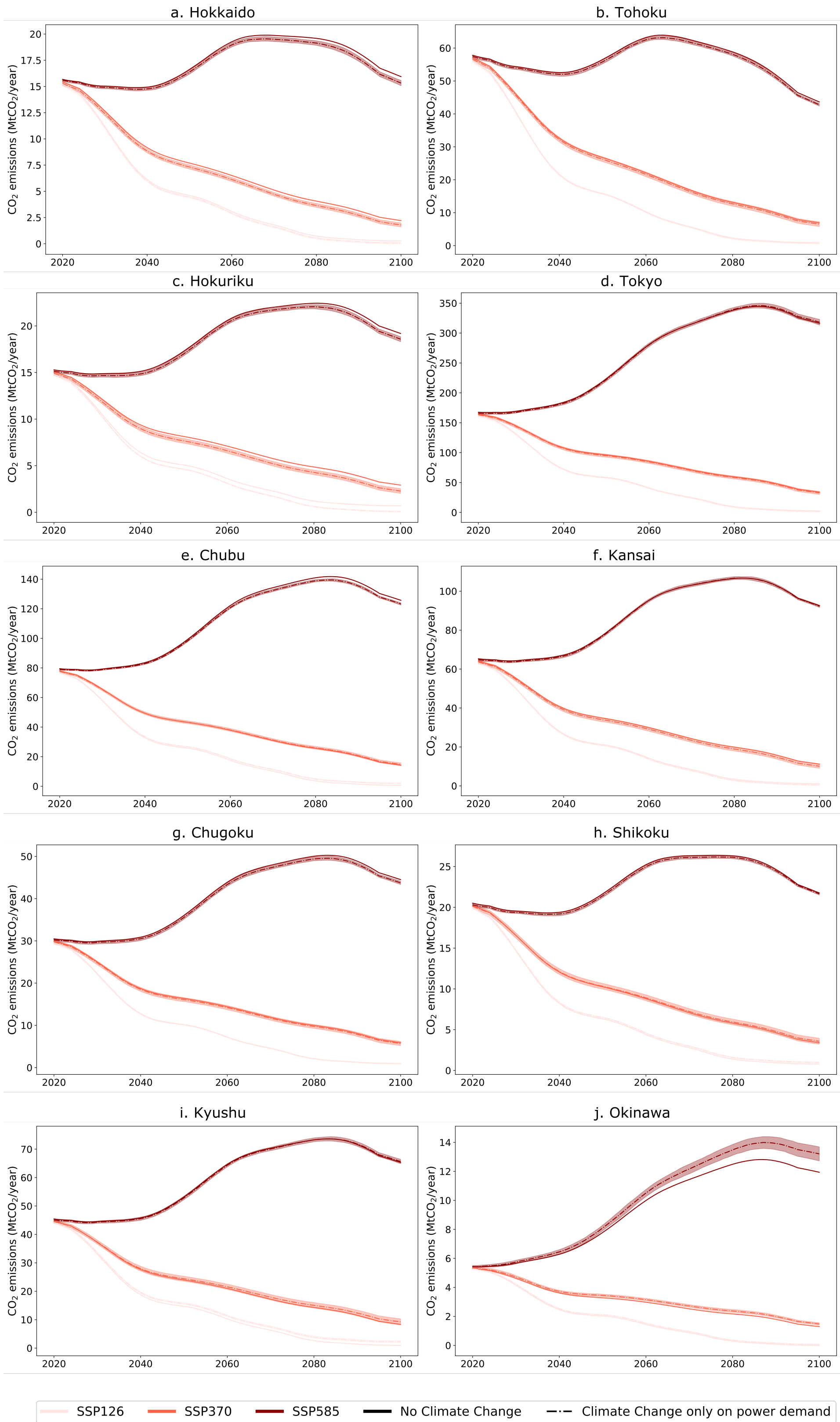

Figure S4. Annual CO_2 emissions from power production under SSP126, SSP370, and SSP585, after taking into account the effect of socio-economic factors with the effect of climate change only on power (dashed line) and without climate change (direct line). The shaded area represents the 1-sigma standard deviation from the five climate models for the climate-change effect curves.

S7. Effect of hot and cold periods on the demand

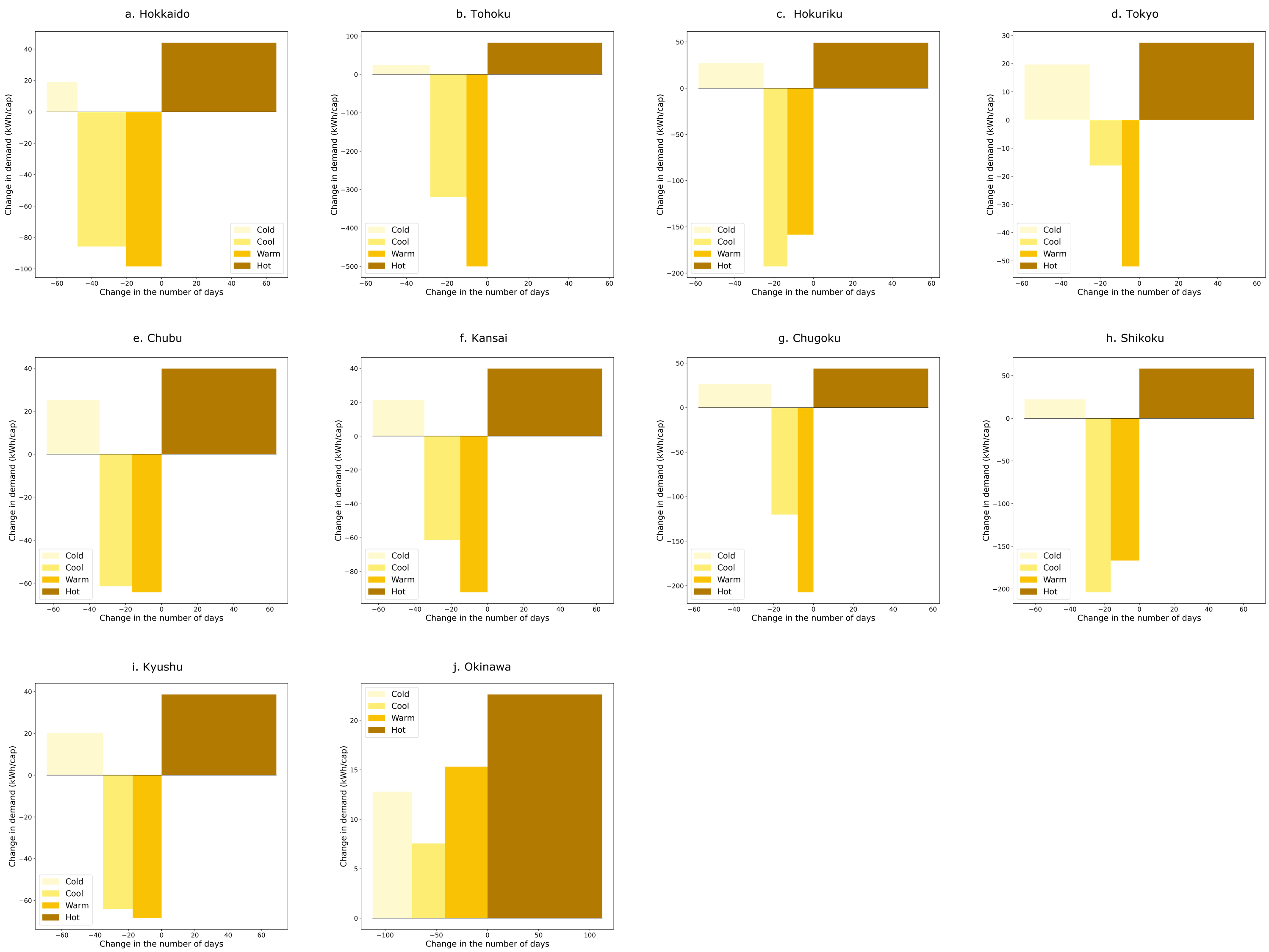

Figure S5. Contribution of cold, cool, warm, and hot days to the change in power demand per capita between the years 2020-2030 and 2090-2100 in four regions (a.) Hokkaido, (b.) Tokyo, (c.) Kansai, and (d.) Okinawa. We represent here the annual average. Cold days are when the temperature is below the 5th percentile. Cool days are when it is between the 5th and the 50th percentile. Warm days are between the 50th and the 95th percentile. Hot days are when it is above the 95th percentile. The percentiles are calculated for each region with their 2016-2020 temperature distribution. The x-axis is the change in the number of days in the four categories, and the y-axis represents the daily change in power demand per capita between the two periods. The area of each rectangle is the average absolute contribution of each category of days to the change in demand. The black dotted line represents the total change in power demand between the two periods.

S8. Monthly change in power demand and carbon intensity

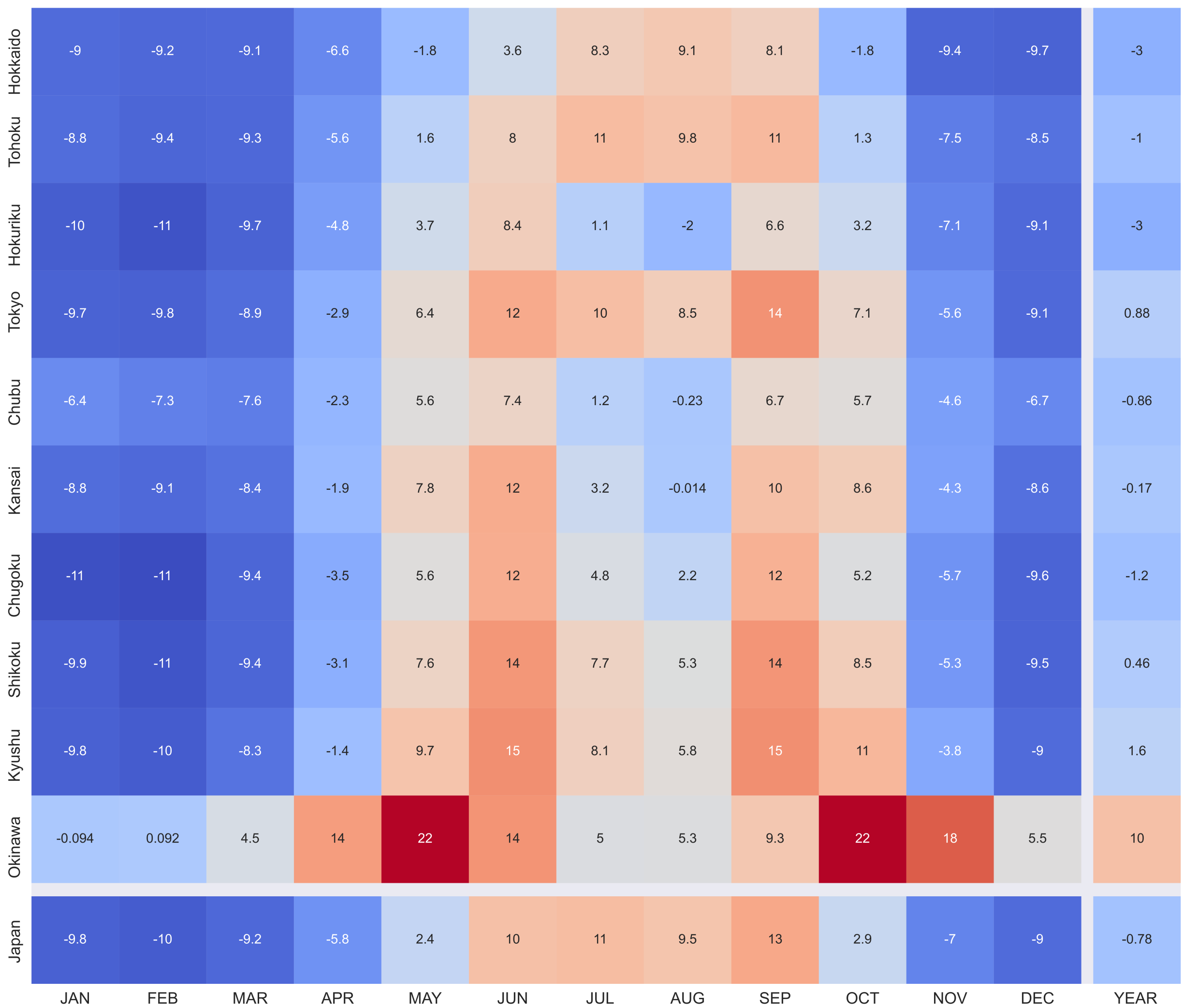

Figure S6a. Monthly and regional changes (in percentage) in power demand between 2020-2030 and 2090-2100 due to climate impacts on future power generation. The mean results of the five models for SSP585 are shown.

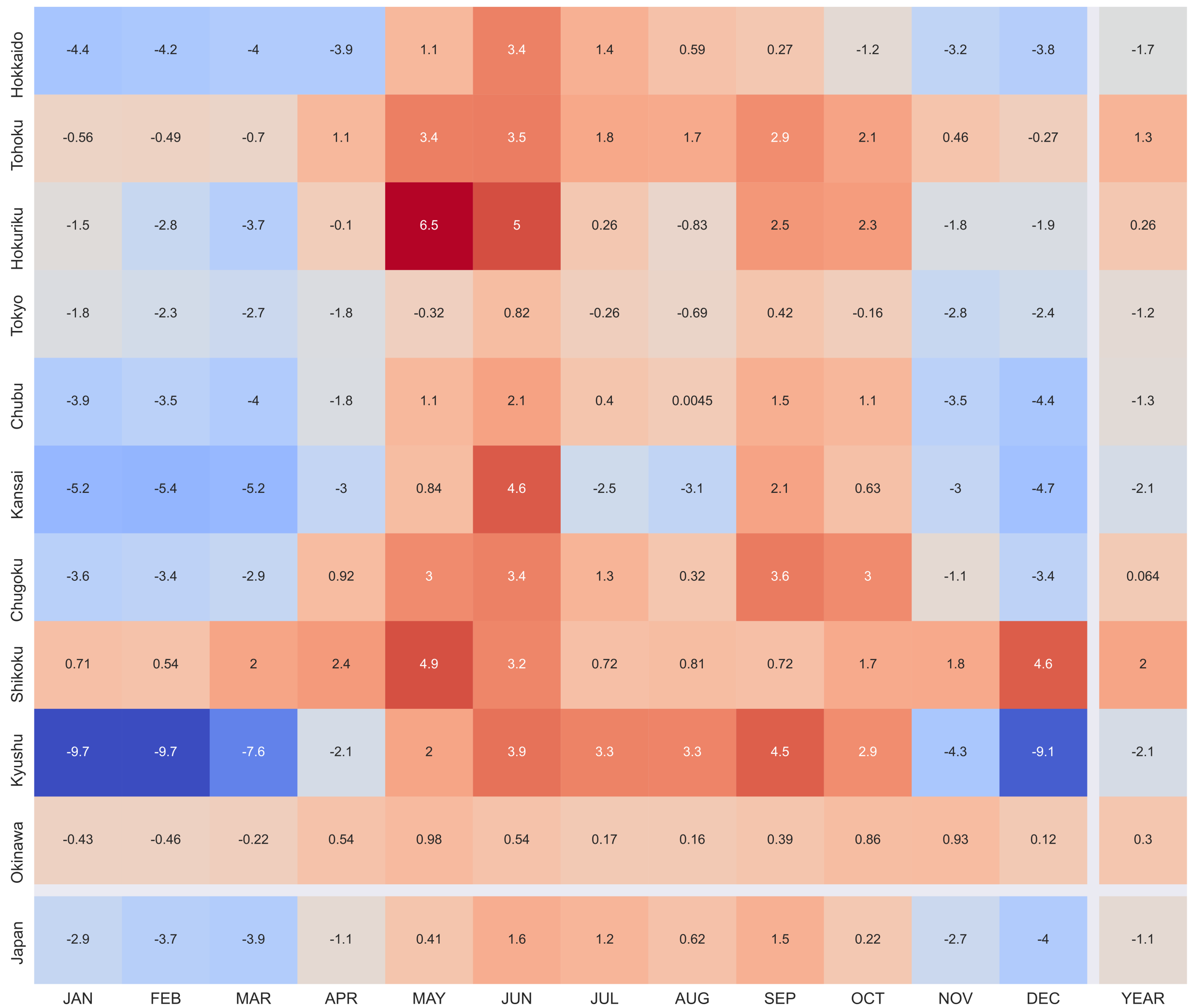

Figure S6b. Monthly and regional changes (in percentage) in carbon intensity between 2020-2030 and 2090-2100 due to climate impacts on future power generation. The mean results of the five models for SSP585 are shown.